Negative thermal expansion in crystals with the delafossite structure: An extended x-ray absorption fine structure study of CuScO$_2$ and CuLaO$_2$

S. I. Ahmed,[*] G. Dalba, P. Fornasini, and M. Vaccari[†]

Dipartimento di Fisica dell'Università di Trento, Via Sommarive 14, I-38050 Povo (Trento), Italy

F. Rocca and A. Sanson[‡]

IFN-CNR, Istituto di Fotonica e Nanotecnologie del Consiglio Nazionale delle Ricerche, Sezione "FBK-CeFSA" di Trento, Via alla Cascata 56/C, I-38050 Povo (Trento), Italy

J. Li and A. W. Sleight

Department of Chemistry, Oregon State University, Corvallis, Oregon 97331, USA

Extended x-ray absorption fine structure has been measured at the K edge of copper in CuScO$_2$ and CuLaO$_2$ to investigate the local origin of negative thermal expansion (NTE) along the c axis. A positive expansion of the Cu-O bond has been measured within the entire temperature interval to be contrasted with the negative expansion of the distance between average atomic positions measured by diffraction; the inadequacy of the riding correction to diffraction data has been evidenced. The weak temperature dependence of the parallel mean-square relative displacement (MSRD) indicates a rather stiff Cu-O bond, while the large perpendicular MSRD measures an intense relative motion of copper with respect to oxygen atoms perpendicular to the c axis. The comparison between the two compounds enlightens the relevance of the correlation of perpendicular motion to quantitatively explain the apparent NTE of the Cu-O bond.

I. INTRODUCTION

Several crystals undergo negative thermal expansion (NTE) within a non-negligible temperature range.[1,2] NTE materials are interesting for technological applications;[3] besides, achieving a complete understanding of the NTE mechanisms represents a challenge for basic research.[4–8] In systems where NTE is of purely vibrational in origin, the macroscopic expansion is the result of a competition between a positive contribution due to a nearest-neighbor bond stretching effect and a negative contribution due a tension effect induced by atomic vibrations perpendicular to some interatomic link (sometimes referred to as "guitar string effect").[5]

Tetrahedrally coordinated crystals often exhibit NTE in limited temperature intervals: the tension effect, attributed to low-frequency transverse acoustic modes with negative Grüneisen parameter,[9] only prevails at low temperatures and is progressively overcome by the stretching effect when temperature increases. Silicon and germanium have very weak NTE in a limited low-temperature interval. Strength and temperature interval of NTE increase with ionicity, reaching the maximum values in CuCl.[10]

Several framework structures exhibit NTE extending over large temperature intervals. The prototypical example is ZrW$_2$O$_8$, where NTE has been measured from 0.3 to 1440 K.[11,12] The structure of ZrW$_2$O$_8$ is made up of WO$_4$ tetrahedra and ZrO$_6$ octahedra joined by oxygen atoms at the corners. The tension effect due to vibrations of corner atoms has been connected to the presence of low-frequency rigid unit modes (RUMs) that cause rotations of the basic polyhedral units.[13,14]

Simpler framework structures undergoing NTE are Cu$_2$O and Ag$_2$O,[15] which share the cuprite structure, made up of two interpenetrating networks of corner sharing undistorted M_4O tetrahedra (M=Cu, Ag), so that each metal atom is linearly coordinated to two oxygen atoms. Strong NTE is exhibited also by the similar framework structure Zn(CN)$_2$.[16]

The framework structures of ZrW$_2$O$_8$, Zn(CN)$_2$ and Ag$_2$O undergo NTE within the full explored temperature interval, with the tension effect always prevailing on the stretching effect. Cu$_2$O exhibits a behavior similar to the zinc-blende CuCl, with the tension effect prevailing only in a limited low-temperature interval. Besides, the low-temperature NTE is stronger in CuCl, where no polyhedral rigid units can be defined, than in the framework structure Cu$_2$O. These properties suggest that a deeper understanding of NTE could be obtained by a comparative study of different structures. A general connection between polyhedral RUMs and NTE cannot be established even for all framework structures.[7,17] A common feature of NTE materials, independent of the presence of polyhedral RUMs, seems to be the relevance of strong vibrations perpendicular to some interatomic bond, such as the linear O-M-O link in cuprites (M=Cu, Ag), or the distorted A-B-A link in zinc blendes.

A systematic experimental investigation of the effects of perpendicular vibrations cannot be based only on the measurement of lattice thermal expansion and atomic thermal factors by Bragg diffraction experiments; studies performed from a local perspective, by means of correlation-sensitive probes such as extended x-ray absorption fine structure (EXAFS),[18] give relevant complementary information.

In powder-diffraction experiments, the extended nature of the incident beam (neutrons or x rays) allows one to calculate an ensemble average over all coherently diffracting domains. The average atomic positions and the anisotropic displacement parameters can be refined; hence, one can
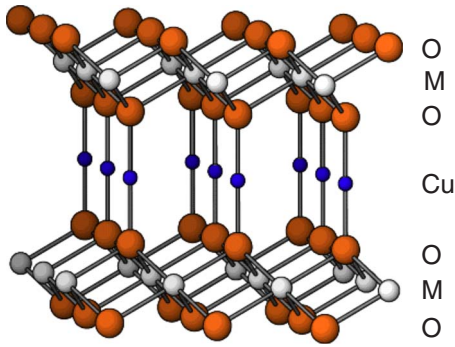
FIG. 1. (Color online) The delafossite structure of CuMO_2 (M =Sc,La). The hexagonal c axis is vertical.

calculate the distance between the average positions of atoms $R=|\langle \mathbf{r}_2 \rangle - \langle \mathbf{r}_1 \rangle|$ and the absolute mean-square displacement (MSD or MSDA) of the different atoms along selected directions.[17,19]

In EXAFS experiments, the photoelectrons sample a unidimensional distribution of distances from the absorbing atom to the atoms of a few neighboring coordination shells. EXAFS is sensitive to the correlation of atomic motion and directly measures the average distance between selected pairs of atoms $\langle r \rangle = \langle |\mathbf{r}_2 - \mathbf{r}_1| \rangle$ and the mean-square relative displacements (MSRDs) parallel to the bond direction.[20,21] The "true" bond length $\langle r \rangle$ and the corresponding thermal expansion measured by EXAFS are larger than the "apparent" bond length R and the corresponding thermal expansion measured by diffraction for selected interatomic bonds, owing to the effect of perpendicular vibrations.[5,17,21] By suitably comparing the results of EXAFS and Bragg diffraction, it is possible to recover the MSRD perpendicular to the bond. An updated account of this procedure is given in Ref. 22; the comparison between EXAFS and Bragg diffraction is thoroughly treated in Sec. II of Ref. 17.

Sensitivity to true bond expansion and possibility of evaluating the perpendicular MSRD make EXAFS a valuable probe of the local origin of NTE. In the NTE systems up to now investigated by EXAFS,[17,23,24] a positive expansion of the nearest-neighbor distance has been found, contrasting the negative expansion of the lattice parameter measured by Bragg diffraction; correspondingly, a strong anisotropy of the MSRD of nearest-neighbor atoms is observed, not only in the linear O-M-O links of cuprites, but also in CuCl, where the temperature factors measured by diffraction are isotropic for symmetry reasons. A comparative synthesis of EXAFS results has been attempted in Ref. 25.

To further investigate on the connection between local dynamics and NTE, a particularly interesting case is represented by several crystals CuMO_2 (M=Al, Sc, In, and La) with the delafossite structure (Fig. 1), which undergo NTE along the c axis in a non-negligible temperature interval.[26] The structure of the CuMO_2 delafossites is characterized by the stacking, along the c axis, of O-M-O layers, where M atoms are octahedrally coordinated to oxygen. The O-M-O layers are connected by Cu cations that are linearly coordinated with two O atoms, with the O-Cu-O link being always parallel to the c axis (Fig. 1). Because of the simple structure around the Cu cations, where no polyhedral units can be

defined, these compounds are particularly suited to investigate on the connection between the NTE of the Cu-O distance along the c axis and the atomic vibrations perpendicular to the c axis; in fact, no polyhedral RUMs can be invoked to explain NTE.

We will here focus the attention on the 3R polymorphs of $CuScO_2$ and $CuLaO_3$, characterized by a ABC stacking of the O-M-O layers. According to powder neutron-diffraction patterns, measured from 30 to 600 K,[26] the a cell parameter undergoes positive expansion within the full temperature interval in $CuScO_2$ and only above about 100 K in $CuLaO_2$; the c parameter contracts from 30 to 300 K in $CuScO_2$ and from 30 to 200 K in $CuLaO_2$ and expands for higher temperatures. The refinement of diffraction patterns has shown that the distance between the average positions of the nearest-neighbor Cu and O atoms decreases from 30 up to 600 K in both compounds, always giving a negative contribution to the expansion along the c axis. The atomic displacement parameters of copper, of purely thermal origin, are anisotropic, with the vibrations perpendicular to the c axis being more intense than the parallel vibrations.

In this paper, we present an EXAFS study of the local structure and dynamics around copper atoms, performed in the temperature range from 10 to 450 K in $CuScO_2$ and from 100 to 450 K in $CuLaO_2$. The aim is to obtain complementary information with respect to diffraction, in order to better understand the relationship between the NTE along the c axis and the perpendicular vibrations of copper atoms. This paper is organized as follows. Sections II and III are dedicated to details on the experiment and the procedures of EXAFS data analysis, respectively. Thermal expansion and mean-square relative displacements obtained from EXAFS are presented in Sec. IV and compared with the corresponding results from neutron diffraction. The results are discussed in Sec. V. Section VI is dedicated to conclusions.

II. EXPERIMENT

The synthesis method for the 3R $CuScO_2$ and $CuLaO_2$ powders has been previously reported.[27,28] The refinement of diffraction patterns indicates that the impurities amount to less than 4% and contain no copper compounds; hence, they give no contribution to the EXAFS spectra measured at the Cu K edge.

Homogeneous samples for EXAFS measurements were prepared by precipitating fine powders of $CuScO_2$ and $CuLaO_2$ on polytetraflouroethylene membranes from suspensions in methyl alcohol. Surface densities of about 11 and 8 mg/cm^2, respectively, allowed us to obtain edge jumps $\Delta \mu x \simeq 1$ at the Cu K edge.

Transmission EXAFS measurements were done at the BM08 (Gilda) beamline of the European Synchrotron Radiation Facility (ESRF) in Grenoble, France. Electron energy and average current were 6 GeV and 190 mA, respectively. The x-ray beam was monochromatized by two parallel silicon crystals with flat (311) reflecting faces, detuned to reduce the harmonics influence. The size of the beam incident on the sample was about 4×1 mm^2. The incoming and outgoing photon fluxes were measured by two ionization cham-
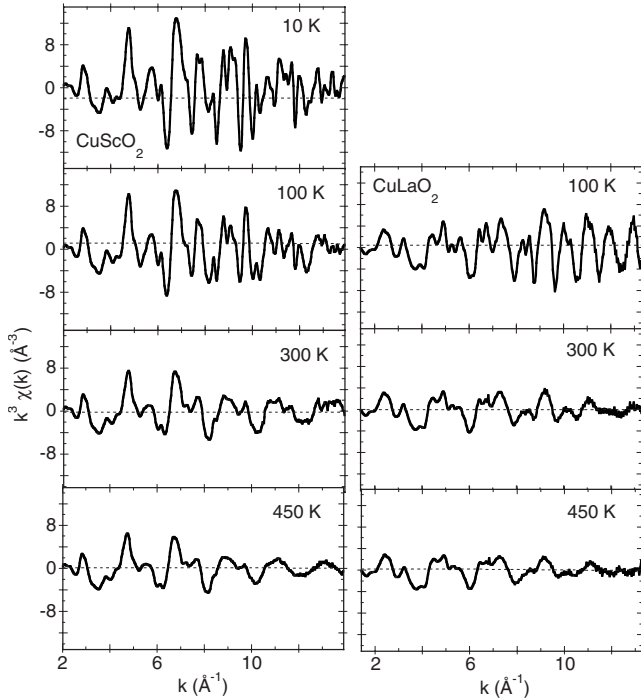
FIG. 2. Weighted EXAFS signals $k^3\chi(k)$ at selected temperatures for $CuScO_2$ (left) and $CuLaO_2$ (right).
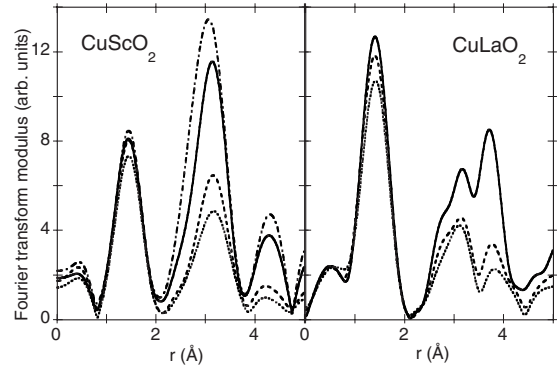

FIG. 3. Fourier-transform modulus of the EXAFS functions of $CuScO_2$ (left) and $CuLaO_2$ (right) at selected temperatures: 10 K (dashed-dotted line), 100 K (continuous lines), 300 K (dashed lines), and 450 K (dotted lines).

bers filled with nitrogen (pressure: 985 mbar) and argon (pressure: 200 mbar), respectively.

The $CuScO_2$ sample was immersed in the He gas atmosphere of a liquid-helium cryostat for measurements below 300 K and attached to the cold/hot finger of a liquid nitrogen cryostat for measurements above 300 K. Measurements on $CuLaO_2$ were done by the liquid-nitrogen cryostat from 100 to 450 K. The temperature control was achieved through an electric heater, controlled by a feedback loop. Thermal stabilization was guaranteed within ± 1 K. The acquisition time was 5 s per point. Two or three spectra were collected at each temperature to allow an evaluation of experimental uncertainty.

III. DATA ANALYSIS

The edges of all spectra were aligned to within 0.1 eV, in order to achieve a resolution on the order of 0.001 Å in distance variations. The EXAFS signal was obtained as $\chi(k)=(\mu-\mu_0)/\mu_0$, where μ is the experimental absorption coefficient and μ_0 is a spline polynomial best fitting the average behavior of μ. The evaluation of the μ_0 curve was not trivial and was attempted by different procedures. The final choice was made, after a careful trial and error procedure for each data file, in order to obtain the best linearity in the subsequent analysis of the phases and amplitudes by the ratio method.

The k-weighted EXAFS functions $k^3\chi(k)$ of the two compounds at selected temperatures are shown in Fig. 2. The overall quality is better for the $CuScO_2$ signal than for the $CuLaO_2$ signal. The higher noise level at high k values for the $CuLaO_2$ signal has to be attributed to the progressive

deterioration with time of the quality of the monochromatized x-ray beam.

The EXAFS functions $k^3\chi(k)$ have been Fourier transformed, with a Gaussian window in the k ranges from 2 to 11.7 Å^{-1} for $CuScO_2$ and from 1.4 to 10.5 Å^{-1} for $CuLaO_2$, in order to separate the contributions of the different coordination shells. The limits of the Fourier-transform intervals were chosen, after a careful trial and error procedure, in order to optimize the subsequent phase and amplitude analysis.

The moduli of Fourier transforms at selected temperatures are shown in Fig. 3. Since the transforms were performed without phase-shift correction, the peak positions are backward shifted with respect to the actual interatomic distances listed in Table I. The peak between about 0.8 and 2.1 Å in the spectra of both compounds is due to the two nearest-neighbor oxygen atoms, linearly connected to the copper atom along the c axis (Fig. 1). The large structure from about 2.1 to 3.8 Å for $CuScO_2$ and from about 2.1 to 4.3 Å for $CuLaO_2$ is due to the contributions of the second, third, and fourth coordination shells (Table I) and to multiple-scattering effects.

The temperature effect is rather weak for the first-shell peak, indicating a relatively stiff link between nearest-neighbor copper and oxygen atoms. The temperature effect is stronger for the outer shells. If one takes into account the inversion of Cu and M atoms in the second and third shells of the two compounds (Table I), a closer look at the outer-

TABLE I. Parameters of the first four coordination shells of Cu in $CuScO_2$ and $CuLaO_2$ at room temperature. Notice the inversion of the Cu and M atoms in the second and third shells of the two compounds (M=Sc,La).

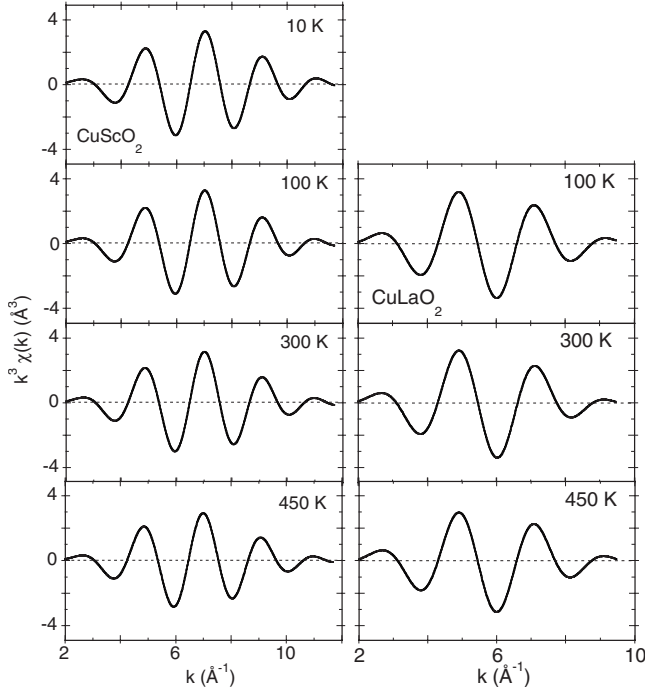| Shell	3R-$CuScO_2$			3R-$CuLaO_2$		
	Atoms		Distance (Å)	Atoms		Distance (Å)
1	2	O	1.83	2	O	1.82
2	6	Cu	3.22	6	La	3.61
3	6	Sc	3.40	6	Cu	3.83
4	12	O	3.69	12	O	4.27

FIG. 4. Fourier-filtered EXAFS signals $k^3\chi(k)$ at selected temperatures for the Cu-O distance in $CuScO_2$ (left) and $CuLaO_2$ (right).

shell structures in Fig. 3 reveals that the temperature effect is stronger for the Cu-Cu distances (in the plane perpendicular to the c axis) than for the Cu-Sc or Cu-La distances.

A careful quantitative analysis was performed for the Cu-O first shell, whose contribution was singled out by back transforming to k space the corresponding peak of Fig. 3. The first-shell EXAFS signals $k^3\chi(k)$ of the two compounds at selected temperatures are shown in Fig. 4. The first-shell EXAFS can be interpreted within the single-scattering approximation and was quantitatively analyzed by the *ratio method* within the cumulant expansion approach.[22,24,29–33]

Basically, the cumulant approach consists in parametrizing the distribution $\rho(r)$ of interatomic distances in terms of its cumulants C_i^*; the lowest-order cumulants have a well-defined physical meaning: C_1^* corresponds to the mean value $\langle r \rangle$ of the distribution, C_2^* corresponds to its variance, and C_3^* measures the asymmetry. The EXAFS function of one coordination shell can in turn be parametrized in terms of the cumulants C_i of an effective distribution $P(r,\lambda) = \rho(r)\exp(-2r/\lambda)/r^2$, where λ is the photoelectron mean-free path,

$$\chi(k) = (S_o^2/k)N|f(k,\pi)|\exp(C_o - 2k^2C_2 + 2k^4C_4/3\cdots)$$
$$\times \sin[2kC_1 - 4k^3C_3/3\cdots + \phi(k)], \quad (1)$$

where S_0^2 is a factor taking into account intrinsic inelastic effects, N is the coordination number, $|f(k,\pi)|$ is the modulus of the backscattering amplitude, and $\phi(k)$ is the total phase shift. The cumulants C_i^* and C_i of the real and effective distributions are connected by well-established relations.

The ratio method consists in separately comparing the phases and amplitudes of the EXAFS signals at different

temperatures T with phases and amplitudes of the spectrum at the lowest temperature T_0 (here, $T_0 = 10$ K for $CuScO_2$ and 100 K for $CuLaO_2$). The procedure cancels the unknown quantities $|f(k,\pi)|$, $\phi(k)$, and S_0^2 and allows one to obtain accurate relative values of the cumulants of the real distribution, $\delta C_i^* = C_i^*(T) - C_i^*(T_0)$.

In the present case of delafossites, phase differences and logarithms of amplitude ratios of all pairs of data files could reasonably be fitted by straight lines in a convenient k^2 interval that corresponds to truncating the cumulant expansion at the third order. Taking into account the third cumulant (asymmetry of the distribution) is essential to get accurate relative values of the first cumulant (average value of the distribution).

The relative values of the first cumulant obtained by the ratio method directly give the sought bond thermal expansion. Absolute values of the second cumulant (variance of the distribution, often referred to as EXAFS Debye-Waller exponent) were evaluated by vertically shifting the experimental relative values in order to obtain the best average agreement with the correlated Einstein model

$$C_2^*(T) = \frac{\hbar}{4\pi\mu\nu}\coth\left(\frac{\hbar\pi\nu}{k_BT}\right) \quad (2)$$

(μ is the reduced mass of absorber and backscatterer atoms) that best fits their temperature dependence, according to a well-established procedure.[34–36] The Einstein approximation can appear rather crude when compared with the expression of the second cumulant as a sum over all normal modes of the crystal;[36,37] it is, however, a matter of experience that the temperature dependence of the second cumulant is satisfactorily fitted by an Einstein model within the current experimental uncertainties,[22,38] and a good agreement has been found also with *ab initio* calculations.[39] This fact is not surprising since at high temperatures the Einstein model asymptotically tends to the linear classical behavior, while at low temperatures the second cumulant is by far less sensitive to the peculiarities of the model than the specific heat. An evaluation of the residual error introduced by the Einstein model has been recently attempted by simulations performed on realistic densities of vibrational states;[40] the typical errors are negligible for the purposes of the present work. The usefulness of parametrizing the second cumulant by one Einstein frequency will be made clear below.

The uncertainties in evaluating the background μ_0 (see above) are particularly relevant in the analysis of the first-shell signal, in view of the low frequency (short interatomic Cu-O distance) and the limited useful k range (backscattering amplitude of the light oxygen atoms). The cumulant values were thus evaluated by averaging the results from different pairs of data files and different fitting intervals; the corresponding error bars take into account both experimental and data analysis uncertainties.

IV. RESULTS

From the EXAFS analysis, relevant information was obtained on: (a) the temperature dependence of the first cumulant of the distribution of distances, $\delta C_1^* = \delta\langle r \rangle$, that corre-
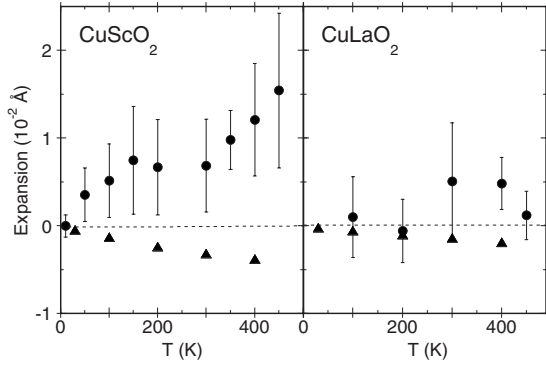
FIG. 5. Expansion of the nearest-neighbor Cu-O bond as measured by EXAFS (circles), compared with the variation of the distance between average positions of the Cu and O atoms (triangles), determined from neutron-diffraction measurements (Ref. [26]).

FIG. 6. Parallel MSRDs $\langle \Delta u_{\parallel}^2 \rangle$ (squares) and perpendicular MRSDs divided by 2 ($\langle \Delta u_{\perp}^2 \rangle / 2$) (diamonds) for the Cu-O distance in $CuScO_2$ (left) and in $CuLaO_2$ (right). The dashed lines are the best-fitting Einstein models.

sponds to the thermal expansion of the Cu-O bond and (b) the second cumulant C_2^* that corresponds to the mean-square relative displacement $\langle \Delta u_{\parallel}^2 \rangle$ of the Cu-O pair of atoms along the c axis.

A. Thermal expansion

The Cu-O bond thermal expansion $\delta C_1^* = \delta \langle r \rangle$ determined from EXAFS is shown in Fig. 5 (circles) for both studied compounds. For $CuLaO_2$, to compensate the fact that the reference was at the relatively high temperature of 100 K, the data were upward shifted, so that the best fitting straight line goes through zero at $T=0$ K. The expansion of the distance R between the average positions of the copper and oxygen atoms, as determined from neutron-diffraction measurements,[26] is shown by triangles.

In spite of the rather large error bars and the scatter of the $CuLaO_2$ data, two main conclusions can be drawn from Fig. 5: the expansion measured by EXAFS is positive for both compounds, and the positive expansion is stronger for the compound that exhibits the stronger apparent negative expansion, say $CuScO_2$. A similar behavior—a positive expansion of the true bond length measured by EXAFS or diffuse scattering and a negative expansion of the apparent bond length measured by Bragg diffraction—has been found also in other systems, such as quartz,[41] the cuprites Cu_2O and Ag_2O,[17] the related compound $Zn(CN)_2$,[16] and the zinc-blende CuCl.[24] Also, for the isostructural cuprites Cu_2O and Ag_2O, like for the delafossites of the present study, the positive bond expansion is stronger for the compound, Ag_2O, that exhibits the stronger apparent negative expansion.

B. Mean-square relative displacements

The parallel MSRD is defined as[20,33]

$$\langle \Delta u_{\parallel}^2 \rangle = \langle [\hat{R} \cdot (\mathbf{u}_b - \mathbf{u}_a)]^2 \rangle = \langle (\hat{\mathbf{R}} \cdot \mathbf{u}_a)^2 \rangle + \langle (\hat{\mathbf{R}} \cdot \mathbf{u}_b)^2 \rangle$$
$$- 2\langle (\hat{\mathbf{R}} \cdot \mathbf{u}_a)(\hat{\mathbf{R}} \cdot \mathbf{u}_b) \rangle, \quad (3)$$

where $\mathbf{u}_a$ and $\mathbf{u}_b$ are the instantaneous displacements of the absorber and backscatterer atoms, respectively, and $\Delta\mathbf{u} = \mathbf{u}_b - \mathbf{u}_a$. The parallel MSRD is thus the average squared projec-
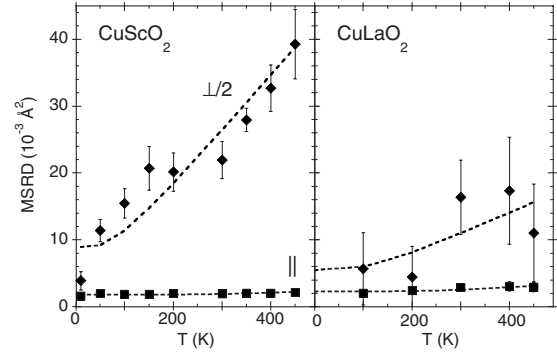
tion of $\Delta\mathbf{u}$ along the bond direction. The first two terms on the second equality of Eq. (3) correspond to the uncorrelated MSDs along the bond direction, $U_{\parallel}^a = \langle (\hat{\mathbf{R}} \cdot \mathbf{u}_a)^2 \rangle$ and $U_{\parallel}^b = \langle (\hat{\mathbf{R}} \cdot \mathbf{u}_b)^2 \rangle$, such as that measured by diffraction. The last term is the parallel displacement correlation function (DCF).[20] The parallel MSRD corresponds, to a good approximation, to the second cumulant C_2^* and is directly measured by EXAFS.

The perpendicular MSRD $\langle \Delta u_{\perp}^2 \rangle$ is the average squared projection of $\Delta\mathbf{u}$ in the plane perpendicular to the bond direction. The relation connecting the distance R measured by diffraction and the distance $\langle r \rangle$ measured by EXAFS is[21,22]

$$R = \langle r \rangle - \langle \Delta u_{\perp}^2 \rangle / 2R_0. \quad (4)$$

The values of $\langle \Delta u_{\perp}^2 \rangle$ have been obtained from the difference $\langle r \rangle - R$, making use of an Einstein model tailored for the perpendicular MSRD [Eq. (2), where μ is substituted by $\mu/2$].[37]

Parallel and perpendicular MSRDs for the Cu-O distance in both compounds are shown in Fig. 6 (the perpendicular MSRD values are divided by 2 to give the projection along one direction). The parallel MSRDs are compared, with an enlarged vertical scale, in Fig. 7. Notwithstanding the error bars, rather large in particular for $CuLaO_2$, two main qualitative conclusions can be drawn: (a) the perpendicular MSRDs are much larger than the parallel MSRDs, indicating
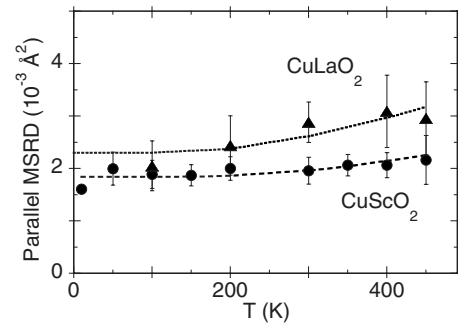

FIG. 7. Parallel MSRDs $\langle \Delta u_{\parallel}^2 \rangle$ in $CuScO_2$ (circles) and in $CuLaO_2$ (triangles). The dotted and dashed lines are the corresponding best-fitting Einstein models.

TABLE II. Parameters describing the temperature dependence of the A-O (A = Cu, Ag) parallel and perpendicular MSRDs in CuScO$_2$ and CuLaO$_2$ (this work) and in Cu$_2$O and Ag$_2$O (Ref. 17). The two last lines list the coefficients of apparent and true bond thermal expansions at low temperatures.

	CuLaO$_2$	CuScO$_2$	Cu$_2$O	Ag$_2$O
$\nu_\parallel$ (THz)	17.2 ± 0.2	21.5 ± 2	14.9	10.2
$\nu_\perp$ (THz)	7.0 ± 0.1	4.4 ± 0.2	7.4	2.9
$k_\parallel$ (eV/Å^2)	15.5 ± 0.3	24.2 ± 4	11.6	5.9
$k_\perp$ (eV/Å^2)	2.6 ± 0.1	1.0 ± 0.2	2.9	0.5
$\xi = k_\parallel / k_\perp$	6.0 ± 0.3	24.2 ± 6	4.1	11.8
α_{app} (10^{-6} K^{-1})	-2.3	-5.5	-2.4	-10.4
α_{true} (10^{-6} K^{-1})	$+9$	$+16$	$+7.5$	$+35$

a strong anisotropy of relative vibrations, and (b) the anisotropy is stronger for CuScO$_2$ than for CuLaO$_2$.

Fitting Einstein models to the MSRDs allows one to parametrize their temperature dependences by one parameter, the Einstein frequency, to which a physical meaning can be attributed. In fact, the Einstein frequencies $\nu_\parallel$ and $\nu_\perp$ can be connected to effective force constants[25] $k_\parallel = 4\pi^2 \nu_\parallel^2 \mu$ and $k_\perp = 4\pi^2 \nu_\perp^2 \mu$ (μ is the reduced mass) that depend on the average effect of all interatomic interactions on a given atomic pair (the effective force constants should not be confused with the usual Born–von Karman force constants). The Einstein frequencies best fitting the temperature dependencies of the MSRDs in delafossites, and the corresponding force constants, are listed in Table II, together with the values found for Cu$_2$O and Ag$_2$O.[17]

C. Correlation

According to Eq. (3), from the difference between the MSRDs and the sum of the uncorrelated MSDs of a pair of atoms, one can measure the correlation of their vibrational motion, in both parallel and perpendicular directions.[17,20,21,24] The actual extent of correlation cannot be obtained solely from diffraction measurements; from the MSD values one can anyway determine the lower and upper bounds to correlation, corresponding to movements perfectly in phase and perfectly in opposition of phase.[17,42]

The MSDs of both copper and oxygen atoms in CuScO$_2$ and CuLaO$_2$ have been determined from neutron-diffraction spectra.[26] Some negative values at low temperatures have been attributed to the strong correlation with the background parameters in the refinement procedure. To obtain positive values suitable to be compared with the EXAFS MSRDs, we fitted the temperature dependence of all MSDs to Einstein models [Eq. (2)] where the reduced mass μ is substituted by the mass m. The lower and higher possible values of MSRDs, obtained from the MSDs according to the procedure of Refs. 17 and 42, are shown in Fig. 8 as up and down triangles, respectively. The comparison with the actual experimental MSRDs (squares) shows that the motion of copper and oxygen atoms is strongly correlated along the c axis in both compounds; the correlation in the perpendicular di-
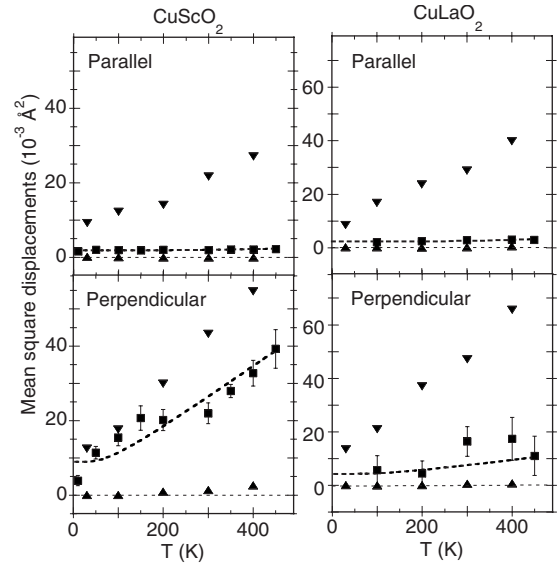

FIG. 8. Parallel MSRD $\langle \Delta u_\parallel^2 \rangle$ (squares in the upper panels) and perpendicular MSRD $\langle \Delta u_\perp^2 \rangle / 2$ (squares in the lower panels) of the Cu-O distance in CuScO$_2$ (left) and CuLaO$_2$ (right) compared with the corresponding lower and upper bounds (up and down triangles, respectively), calculated from the MSDs measured by neutron diffraction.

rection is instead weaker and quite different for the two compounds.

V. DISCUSSION

Let us start the discussion from a comparison between the behavior of the delafossite structure of CuScO$_2$ and CuLaO$_2$ and the cuprite structure of Cu$_2$O.[17] Both structures share the linear O-Cu-O coordination that favors the perpendicular motion of copper atoms and gives rise to a strong NTE contribution. However, in delafossites the expansion of the distance between the average positions of copper and oxygen atoms is not directly proportional to the expansion of the lattice parameters, as it happens instead in Cu$_2$O. Besides, while the thermal expansion is isotropic in the cubic structure of cuprite, a strong anisotropy characterizes delafossites.

According to Bragg diffraction results,[26] the expansion of the c parameter in delafossites results from two contributions, one always positive of the O-Sc-O or O-La-O layer and one always negative of the O-Cu-O link, with the latter prevailing at low temperatures and the former prevailing at high temperatures. By contrast, in Cu$_2$O the expansion of the O-Cu-O link is negative at low temperatures and positive at high temperatures, like the expansion of the cubic lattice parameter. The different behavior can be connected to the different structure: in delafossites, all O-Cu-O links are aligned along the c axis and are perpendicular to the O-Sc-O or O-La-O layer, so that the motion of Cu atoms perpendicular to the O-Cu-O link is weakly constrained. In Cu$_2$O, each oxygen atom is tetrahedrally coordinated to four copper atoms; the O-Cu-O links have different orientations and the motion of Cu atoms perpendicular to the O-Cu-O links is differently constrained by the crystal structure.

The cuprite structure can be considered as formed by two interpenetrating networks of corner-sharing Cu_4O tetrahedra; the presence of tetrahedral structural units could in principle lead to attribute the NTE to the effect of rigid unit modes (RUMs), although this hypothesis seems not supported by experimental results.[17] For $CuScO_2$ and $CuLaO_2$, no polyhedral units can be defined involving copper atoms, so that the crystals with the delafossite structure are particularly suited to study the origin of NTE independently of the presence of RUMs.

The NTE of the Cu-O distance measured by Bragg diffraction[26] is an apparent bond expansion[5] and is related to the large vibrations of the Cu atoms within the plane perpendicular to the c axis. A conservative evaluation of the true expansion of a given bond can be attempted, on the basis solely of diffraction results, by applying the riding motion correction,[42] which assumes that the two atoms move in phase. Actually, the riding correction leads to a weak positive expansion of the Cu-O bond in $CuScO_2$ and a nearly zero expansion in $CuLaO_2$.[26] The true expansion of the Cu-O bond measured by EXAFS is also positive, but much larger than the expansion obtained from the riding correction, at least for $CuScO_2$. The inadequacy of the riding model can be qualitatively understood by comparing the MSRDs measured by EXAFS for $CuScO_2$ and $CuLaO_2$ with their lower and upper bounds determined from diffraction (Fig. 8). In fact, while the Cu and O atoms move in phase along the bond direction (parallel MSRDs, upper panels) in both compounds, their motion within the perpendicular plane (perpendicular MSRDs, lower panels) is only weakly correlated, giving rise to true expansions larger than those expected according to the riding model; this effect is much stronger for $CuScO_2$, where the Cu and O motions are partially in opposition of phase, than for $CuLaO_2$, where the Cu and O motions are partially in phase.

A positive expansion of the true nearest-neighbor bond length has been found in all the NTE materials up to now studied by correlation-sensitive techniques, such as EXAFS and total scattering.[16,17,24,41] Quantitative hints on the vibrational origin of NTE can be obtained by analyzing the parallel and perpendicular MSRDs of different systems and comparing them with the uncorrelated MSDs. Particularly relevant seems to be the anisotropy of relative vibrations, measured by the ratio $\gamma = \langle \Delta u_\perp^2 \rangle / \langle \Delta u_\parallel^2 \rangle$; for perfect isotropy, $\gamma = 2$. The value of γ is temperature dependent and its asymptotic value for $T \to \infty$ has been generally considered.[17,22,24,43] A simpler and more effective procedure[25] is to evaluate the ratio $\xi = k_\parallel / k_\perp$, which is equivalent to the asymptotic value of $\gamma/2$. For perfect isotropy, $\xi = 1$.

The parallel and perpendicular force constants, $k_\parallel$ and $k_\perp$, respectively, and their ratio $\xi = k_\parallel / k_\perp$ for the Cu-O distance in $CuScO_2$, $CuLaO_2$, and Cu_2O and the Ag-O distance in Ag_2O are listed in Table II, together with the values of the apparent and true bond thermal expansion coefficients at low temperature. For all listed compounds, the stronger the apparent NTE, the stronger the positive true bond expansion.

The constant $k_\parallel$ is a measure of the stiffness of the bond against stretching and depends on the extent of the thermal displacements of the pair of atoms, as well as on their cor-

relation. $CuScO_2$ and $CuLaO_2$ are characterized by higher values of $k_\parallel$ than Cu_2O and Ag_2O. The comparison with the uncorrelated MSDs (Fig. 8 in this paper and Fig. 13 in Ref. 17) shows that the motion of metal and oxygen atoms along the bond direction is strongly in phase in delafossites and cuprites. However, while in cuprites the stiffer bond (Cu_2O) undergoes a weaker NTE than the looser bond (Ag_2O), in delafossites the stiffer bond ($CuScO_2$) undergoes a stronger NTE than the looser bond ($CuLaO_2$). The connection between bond stiffness and NTE is not trivial. It is reasonable that the bond stiffness has different values and different effects in the rather constrained structure of cuprite with respect to the layered structure of delafossite, where Cu atoms are quite free to move perpendicularly to the c axis.

Let us now focus our attention on the motion of Cu atoms perpendicular to the c axis in delafossites. Lanthanum atoms are larger than scandium atoms, and correspondingly the Cu-Cu distance is larger in $CuLaO_2$ than in $CuScO_2$ (Table I). The thermal ellipsoids of Cu atoms, measured by Bragg diffraction, are disk shaped;[26] the width of the disks, measuring the absolute motion perpendicular to the c axis, is slightly larger in $CuLaO_2$ than in $CuScO_2$, consistent with the larger Cu-Cu distance. In spite of this, the NTE is stronger in $CuScO_2$ than in $CuLaO_2$. This apparent discrepancy can be explained if one considers the relative perpendicular motion, measured by EXAFS, instead of the absolute motion measured by diffraction. The perpendicular MSRD is much larger in $CuScO_2$ than in $CuLaO_2$ (Fig. 6), and correspondingly the perpendicular force constant is much smaller (Table II). The different behavior of absolute MSDs and relative MSRDs in the two compounds can be explained in terms of different correlation of perpendicular motion: according to Fig. 8, the motion of Cu and O atoms perpendicular to the c axis is partially in phase in $CuLaO_2$ and partially in opposition of phase in $CuScO_2$.

It is thus reasonable to assume that the *relative* perpendicular motion measured by the MSRD, rather than the *absolute* motion measured by the MSD, can quantitatively account for the effect giving rise to the NTE. Alternatively, one can consider the anisotropy of the relative thermal ellipsoids, measured by the ratio $\xi = k_\parallel / k_\perp$. Whether the ratio ξ can be better connected to NTE than the value of the perpendicular force constant $k_\perp$ is a question that requires further investigations on different systems.

VI. CONCLUSIONS

An EXAFS study of the Cu-O distances has been performed in $CuScO_2$ and $CuLaO_2$ as a function of temperature to gain a deeper insight on the local mechanisms of NTE.

(a) While, according to neutron Bragg diffraction, the distance between the average positions of copper and oxygen atoms undergoes negative expansion, the expansion of the Cu-O bond length measured by EXAFS is positive. The difference between EXAFS and Bragg diffraction expansions is due to relative vibrations perpendicular to the Cu-O bond, say perpendicular to the c axis.

(b) The positive expansion of the Cu-O bond length measured by EXAFS is much larger, in both compounds, than

the expansion evaluated, solely from diffraction results, by means of the riding correction.

(c) The bond-stretching effective force constant determined from the parallel MSRD is very large, indicating a stiff Cu-O bond in both compounds. The comparison with Cu_2O suggests, however, that no direct connection can be established between NTE and bond stiffness for crystals with different structures.

(d) The analysis of the vibrations perpendicular to the Cu-O bond suggests that the relative MSRD can be better connected to NTE than the absolute MSD. The phase relationship between vibrational motions of the two atoms has to be taken into account if a quantitative connection between local dynamics and NTE is sought.

(e) Both the perpendicular force constants $k_\perp$ and the anisotropy ratio $\xi = k_\parallel / k_\perp$ can be correlated with NTE. No definitive assessment can yet be made about the relative merits of the two parameters to connect local dynamics and NTE.

ACKNOWLEDGMENTS

*Present address: Ain Shams University, Cairo, Egypt.

†Present address: ESRF, Grenoble, France.

‡Present address: Dipartimento di Informatica, Università di Verona, Verona, Italy.

[1] G. K. White, Contemp. Phys. **34**, 193 (1993).

[2] J. S. O. Evans, J. Chem. Soc. Dalton Trans. **19**, 3317 (1999).

[3] R. Roy, D. K. Agrawal, and H. A. McKinstry, Annu. Rev. Mater. Sci. **19**, 59 (1989).

[4] T. H. K. Barron and G. K. White, *Heat Capacity and Thermal Expansion at Low Temperatures* (Kluwer, New York/Plenum, New York, 1999).

[5] G. D. Barrera, J. A. Bruno, T. H. K. Barron, and N. L. Allan, J. Phys.: Condens. Matter **17**, R217 (2005).

[6] A. W. Sleight, Curr. Opin. Solid State Mater. Sci. **3**, 128 (1998).

[7] J. Tao and A. Sleight, J. Solid State Chem. **173**, 442 (2003).

[8] J. N. Grima, V. Zammit, and R. Gatt, Xjenza **11**, 17 (2006).

[9] T. H. K. Barron, in *Thermal Expansion of Solids*, CINDAS Data Series on Material Properties Vol. I-4, edited by C. Y. Ho (ASM International, 1998).

[10] T. H. K. Barron, J. A. Birch, and G. K. White, J. Phys. C **10**, 1617 (1977).

[11] T. A. Mary, J. S. O. Evans, T. Vogt, and A. W. Sleight, Science **272**, 90 (1996).

[12] N. Duan, U. Kameswari, and A. W. Sleight, J. Am. Chem. Soc. **121**, 10432 (1999).

[13] A. K. A. Pryde, K. D. Hammonds, M. T. Dove, V. Heine, J. D. Gale, and M. C. Warren, J. Phys.: Condens. Matter **8**, 10973 (1996).

[14] V. Heine, P. R. L. Welche, and M. T. Dove, J. Am. Ceram. Soc. **82**, 1793 (1999).

[15] W. Tiano, M. Dapiaggi, and G. Artioli, J. Appl. Crystallogr. **36**, 1461 (2003).

[16] K. W. Chapman, P. J. Chupas, and C. J. Kepert, J. Am. Chem. Soc. **127**, 15630 (2005).

[17] A. Sanson, F. Rocca, G. Dalba, P. Fornasini, R. Grisenti, M. Dapiaggi, and G. Artioli, Phys. Rev. B **73**, 214305 (2006).

[18] D. C. Koningsberger and R. Prins, *X-ray Absorption: Principles and Application Techniques of EXAFS, SEXAFS, and XANES* (Wiley, New York, 1988).

[19] G. Artioli, in *Energy Modelling in Minerals*, EMU Notes in Mineralogy Vol. 4, edited by C. M. Gramaccioli (Eötvös University Press, Budapest, 2002), pp. 389–405.

[20] G. Beni and P. M. Platzman, Phys. Rev. B **14**, 1514 (1976).

[21] P. Fornasini, J. Phys.: Condens. Matter **13**, 7859 (2001).

[22] P. Fornasini, S. a Beccara, G. Dalba, R. Grisenti, A. Sanson, M. Vaccari, and F. Rocca, Phys. Rev. B **70**, 174301 (2004).

[23] S. a Beccara, G. Dalba, P. Fornasini, R. Grisenti, A. Sanson, and F. Rocca, Phys. Rev. Lett. **89**, 025503 (2002).

[24] M. Vaccari, R. Grisenti, P. Fornasini, F. Rocca, and A. Sanson, Phys. Rev. B **75**, 184307 (2007).

[25] P. Fornasini, S. I. Ahmed, A. Sanson, and M. Vaccari, Phys. Status Solidi B **245**, 2497 (2008).

[26] J. Li, A. W. Sleight, C. Y. Jones, and B. H. Toby, J. Solid State Chem. **178**, 285 (2005).

[27] J. Li, A. Yokochi, T. G. Amos, and A. W. Sleight, Chem. Mater. **14**, 2602 (2002).

[28] J. Li, A. F. T. Yokochi, and A. W. Sleight, Solid State Sci. **6**, 831 (2004).

[29] G. Bunker, Nucl. Instrum. Methods Phys. Res. **207**, 437 (1983).

[30] G. Dalba, P. Fornasini, and F. Rocca, Phys. Rev. B **47**, 8502 (1993).

[31] J. M. Tranquada and R. Ingalls, Phys. Rev. B **28**, 3520 (1983).

[32] E. D. Crozier, J. J. Rehr, and R. Ingalls, in *X-ray Absorption*, edited by D. C. Koningsberger and R. Prins (Wiley, New York, 1988), Chap. 9, pp. 373–442.

[33] P. Fornasini, F. Monti, and A. Sanson, J. Synchrotron Radiat. **8**, 1214 (2001).

[34] E. Sevillano, H. Meuth, and J. J. Rehr, Phys. Rev. B **20**, 4908 (1979).

[35] A. I. Frenkel and J. J. Rehr, Phys. Rev. B **48**, 585 (1993).

[36] G. Dalba and P. Fornasini, J. Synchrotron Radiat. **4**, 243 (1997).

[37] M. Vaccari and P. Fornasini, J. Synchrotron Radiat. **13**, 321 (2006).

[38] J. Purans *et al.*, Phys. Rev. Lett. **100**, 055901 (2008).

[39] D. Strauch, P. Pavone, N. Nerb, K. Karch, W. Windl, G. Dalba, and P. Fornasini, Physica B **219-220**, 436 (1996).

[40] A. Sanson, J. Synchrotron Radiat. **15**, 514 (2008).

[41] M. G. Tucker, M. T. Dove, and D. A. Keen, J. Phys.: Condens. Matter **12**, L425 (2000).

[42] W. R. Busing and H. A. Levy, Acta Crystallogr. **17**, 142 (1964).

[43] G. Dalba, P. Fornasini, R. Grisenti, and J. Purans, Phys. Rev. Lett. **82**, 4240 (1999).